Acta Polytechnica **54**(5):358–362, 2014
doi:10.14311/AP.2014.54.0358

available online at http://ojs.cvut.cz/ojs/index.php/ap

EFFECTIVE FRACTURE ENERGY OF ULTRA-HIGH-PERFORMANCE FIBRE-REINFORCED CONCRETE UNDER INCREASED STRAIN RATES

Radoslav Sovják*, Jana Rašínová, Petr Máca

Czech Technical University in Prague, Faculty of Civil Engineering, Experimental Centre, Thákurova 7, 166 29 Prague, Czech Republic

* corresponding author: sovjak@fsv.cvut.cz

Abstract. The main objective of this paper is to contribute to the development of ultra-high-performance fibre-reinforced concrete (UHPFRC) with respect to its effective fracture energy. This paper investigates the effective fracture energy, considering various fibre volume fractions and various strain rates. It is concluded that the effective fracture energy is dependent on the strain rate. In addition, it is found that higher fibre volume fractions tend to decrease the sensitivity of UHPFRC to increased strain rates.

Keywords: Effective fracture energy; UHPFRC; quasi-static loading; increased strain rates; micro fibres; fibre volume fraction.

1. Introduction

Ultra-high-performance fibre-reinforced concrete (UHPFRC) is an advanced cementitious composite with enhanced mechanical and durability properties. Nowadays, UHPFRC is not considered as an alternative to conventionally used materials, but it outperforms conventionally used concretes. The reasons for the present situation are the higher initial costs, and also a certain inertia in the present-day building industry that has led to the continued use of conventional concretes. The application of UHPFRC is therefore limited to special applications such as energy absorption facade panels and key elements of building structures that may be exposed to increased loading rates resulting from earthquakes, impacts or blasts [1, 2]. In the event of increased loading rates, a large deformation of the structural member is expected, while the exposed member is required to continue to possess some residual capacity to carry the load. The capacity of the member to absorb the energy can be quantified via the effective fracture energy, which determines the overall energy that a material can absorb per square meter. The energy absorption capacity is the main material property that benefits from fibre reinforcement. The effective fracture energy (G_f) is a key parameter for evaluating the ability of a material to withstand an increased loading rate and also to redistribute the load from the exposed structure to its surrounding parts. In addition, different behaviour of UHPFRC in terms of G_f can be expected at higher loading rates, as the action is shorter by a magnitude than for quasi-static loading (see Figure 1).

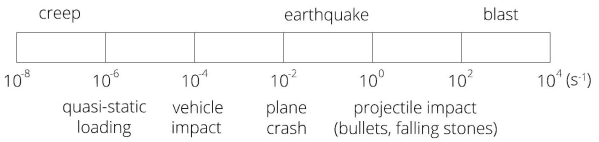

Figure 1. Strain rates for various load events.

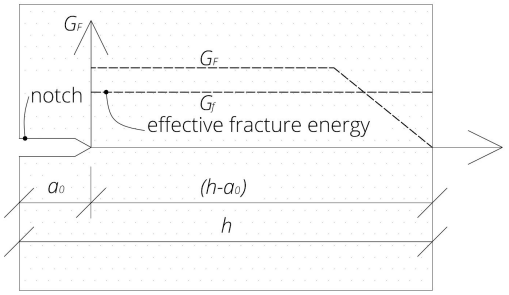

Figure 2. Effective fracture energy of a notched specimen.

2. Effective fracture energy

The effective fracture energy (G_f) of a material is defined as the energy required to open a unit crack surface area. G_f is governed by the tensile mechanism of the material, and represents the amount of energy consumed when a crack propagates through the beam. The fracture energy is expressed as the work of external forces acting on the beam related to the actual depth of the crack. The overall work of the external forces related to the final crack depth is considered as the average fracture energy, the so-called effective fracture energy (Figure 2).

The effective fracture energy (G_f) is strain rate dependent, and it is assumed that G_f also increases with increasing strain rate. This dependence is usually described by the dynamic increase factor (DIF), which expresses the ratio of G_f measured under increased strain rate loading conditions to G_f measured under

Fibre content	1 %	2 %	3 %
Cement CEM I 52.5R		800	
Silica fume		200	
Silica powder		200	
Water		176	
Superplasticizer		39	
Fine sand 0.1/0.6 mm		336	
Fine sand 0.3/0.8 mm	720	640	560
Fibres 0.22 × 13 mm	80	160	240

TABLE 1. Mixture design of the UHPFRC used in this study (all values are in kg/m^3).

FIGURE 3. Micro fibres used in this study.

quasi-static loading conditions:

$$DIF_{G_f} = \frac{G_f^{\text{increased strain rate}}}{G_f^{\text{quasi-static strain rate}}}.$$

G_f was determined in this study on the basis of recommendations given by the RILEM Technical Committee [3] and also by other studies [4, 5]:

$$G_f = \frac{W_f + mgu_u}{b(h - a_0)},$$

where G_f is the effective fracture energy, W_f is the work of external forces (i.e., the area beneath the L–D diagram), and mgu_u is the contribution of the weight of the beam. In detail, m is the weight of the beam, g is gravity acceleration, u_u is the ultimate deflection of the beam, b is the width of the beam, h is the height of the beam, and a_0 is the height of the notch.

3. MATERIAL

The UHPFRC tested in this study was developed on the basis of components widely available in the Czech Republic (see Table 1). The material design process has been fully described elsewhere [6–8]. Briefly, the UHPFRC was mixed in conventional mixers, and the beams were cured in water tanks. The mixture contained a high volume of cement and silica fume, and the water-to-binder ratio was 0.18. In this study the strain rate and the fibre volume fraction (i.e., the fibre content) were selected as the main test variables. The high-strength steel fibres used in this study were 13 mm in length and 0.22 mm in diameter (see Figure 3). The fibres were straight, with tensile strength of 2800 MPa. The high tensile strength of the fibres was chosen in order to achieve the pull-out failure mode. The pull-out failure mode (see Figure 4a) is a much more energy-consuming mode than the fibre failure mode (see Figure 4b). Straight fibres also provided a good trade-off between workability and the mechanical properties of the resulting mixture.

Fibre content	1 %	2 %	3 %
Compressive strength	150	152	150
Tensile strength	7.8	9.9	11.7
Modulus of rupture	15.8	25.6	33.8
Splitting tensile strength	14.9	20.5	26.6
Modulus of elasticity (in GPa)	45.1	56.3	51.5

TABLE 2. Mechanical properties of the UHPFRC used in this study (all values are in MPa).

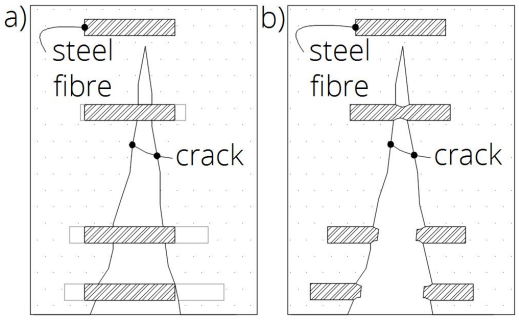

FIGURE 4. a) Pull-out failure mode. b) Fibre failure mode.

As shown in Table 2, the compressive strength measured on cylinders 200 mm in height and 100 mm in diameter was around 150 MPa. The compressive strength did not vary with increasing fibre content. However, the uniaxial tensile strength, the modulus of rupture and the splitting tensile strength showed linear dependence on the actual fibre content (see Table 2). The maximum tensile strength was determined to be 11.7 MPa when the fibre content was 3 % by volume [9].

The UHPFRC mixture was placed in moulds along the length of the beam, and this caused the fibres to be aligned along the length of the beam [10]. This led to fibre alignment in the direction of the tensile stress. No other technique was used to align the fibres. All beams were tested after 28 days from casting in order

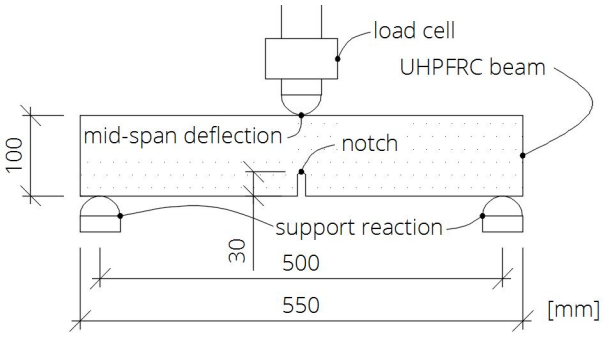

Figure 5. Experimental setup.

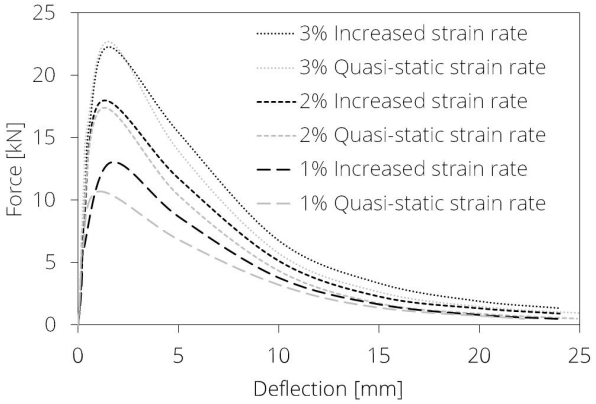

Figure 6. Load–deflection diagrams for UHPFRC beams under various strain rates and with various fibre contents.

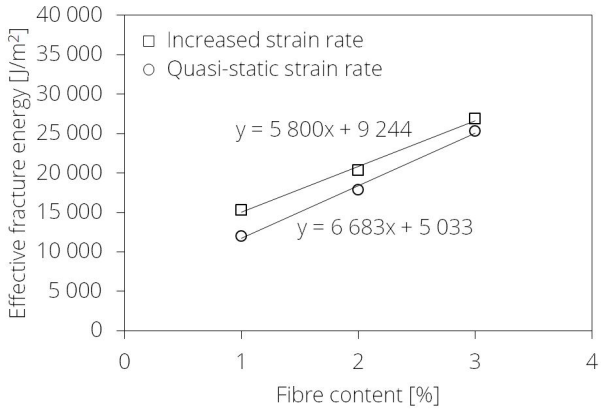

Figure 7. Development of the effective fracture energy.

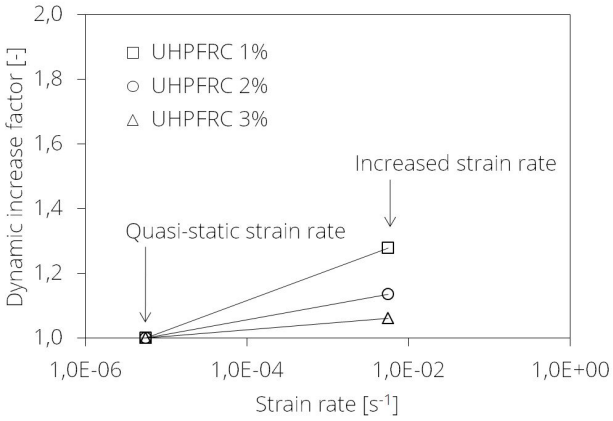

Figure 8. Development of the dynamic increase factor.

to avoid the effect of ageing, which may also influence the results [11].

4. Experimental program

Experiments were performed on beams $100 \times 100 \times 550$ mm in size with a clear span of 500 mm. The beams had a notch in their bottom edge which was 30 mm in height and 5 mm in width (Figure 5). Three different fibre volume fractions were tested covering 1 %, 2 % and 3 % of the fibre volume content. Each fibre volume fraction was tested under quasi-static conditions and under increased strain-rate conditions. Quasi-static conditions were simulated by a deformation controlled test with a speed of the cross-head of 0.2 mm/min. This speed corresponded to a strain rate of $5.6 \times 10^{-6}\,\mathrm{s}^{-1}$, which is considered as the quasi-static strain rate [12, 13]. An increased strain-rate was simulated by the greatest possible motion of the cross-head of the hydraulic testing machine used in this study. The cross-head developed a speed of 200 mm/min, corresponding to a strain rate of $5.6 \times 10^{-3}\,\mathrm{s}^{-1}$. This level of strain rate is typical for dynamic loading, e.g., for earthquakes. During the experimental program, the force acting on the beam and the deflection measured by two LVDT (linear variable differential transformer) sensors was recorded with 5 Hz and 1 kHz frequency during quasi-static loading and increased strain rate loading, respectively. Steel yokes were implemented in the experimental setup as mounts for the LVDT sensors, in order to subtract the settlement of the supports from the measured deflections [14].

5. Results and discussion

Load–deflection (L–D) diagrams were plotted for all beams, including various fibre volume fractions tested under various strain rates. Three beams were tested for all fibre contents and for both strain rates, making a total of 18 tested beams. The ZUZ-200 hydraulic testing machine with a closed loop deformation control system with a maximal capacity of 100 kN was used for both loading rates. The tests were deformation controlled, based on the movement of the crosshead, which was either 0.2 mm/min for quasi-static loading or 200 mm/min for the increased strain rate (see Figure 6).

Several authors have suggested that for low strain rates the fracture energy is constant, and is therefore not dependent on the loading rates [15, 16]. However, in our study it was found that for increasing fibre contents and also for increasing strain rates the effective fracture energy also increases (see Figure 7). This is because in the case of quasi-static loading the crack propagates along the line with the least resis-

G_f [J/m^2]			
Fibre content	**Strain rate**		
	$5.6 \times 10^{-6}\,\mathrm{s}^{-1}$	$5.6 \times 10^{-3}\,\mathrm{s}^{-1}$	DIF
1 %	12000 (2100)	15300 (3200)	1.28
2 %	17900 (1200)	20300 (1500)	1.13
3%	25300 (700)	26900 (1900)	1.06

TABLE 3. Effective fracture energy of the UHPFRC.

tance, which leads to minimal fracture energy. In the case of increased strain rates, the crack does not have enough time to seek the lowest energy consumption path, and goes straight through the beam, which is a more energy-consuming procedure [17]. Other authors have suggested that the rate effect for low strain rates can also be attributed to viscous effects, which mainly originate due to the presence of free water in voids and in porous structures [18]. For higher fibre contents, the sensitivity to strain rates decreases due to the group effect of fibres that interact together. Denser fibre concentration decreases the pull-out capacity of the fibres, because the matrix surrounding the fibre will not be sufficient to keep the interfacial bonding as strong as in the single pull-out case [17]. When the pull-out capacity is lower, the sensitivity to loading rates is also lower. This is indicated by the dynamic increase factor (DIF), as shown in Table 3 and Figure 8. The effective fracture energy values indicated in Table 3 are averages from three beams. The value in parentheses gives the standard deviation from the tested beams.

6. Conclusions and further outlook

The effective fracture energy was determined on a total of 18 beams, which were tested under various strain rates and with various fibre contents. The fibre volume fraction ranged from 1 % to 3 % by volume, and the strain rate was either $5.6 \times 10^{-6}\,\mathrm{s}^{-1}$ or $5.6 \times 10^{-3}\,\mathrm{s}^{-1}$. The following conclusions can be drawn on the basis of the experimental outcomes derived from this study:

(1.) The effective fracture energy (G_f) increases as the fibre volume fraction increases. Higher scatter in the experimental outcomes was observed for lower fibre contents. The pull-out capacity of the fibre in a higher fibre volume content is lower than the pull-out capacity of the fibre in a lower fibre volume content. Each fibre plays a more significant role in terms of G_f in beams with a lower fibre content, because its pull-out capacity is higher. Thus each mismatch in the fibre distribution in lower fibre contents will scatter the results more.

(2.) G_f is dependent on the strain rates. It was verified experimentally that G_f increases as the strain rate increases. In addition, it was found that higher fibre volume fractions attenuate the dependence of G_f on the strain rate. This is because when there is a higher fibre volume fraction the maximum pull-out capacity on each individual fibre is reduced; its sensitivity to higher strain rates is therefore also reduced.

(3.) Two strain rates were considered in this study, which can both be classified as low strain rates. An increased strain rate was simulated as the maximum speed developed by the hydraulic testing machine. It is important to note that it is a fairly complex and highly time-consuming task to make proper measurements of the effective fracture energy. This is the main reason why no experimental work was performed on other strain rate levels. It is therefore highly desirable to extend the scope of our study presented here, and to verify the effective fracture energy of fibre-reinforced cementitious composites under higher strain rates above $10^{-2}\,\mathrm{s}^{-1}$.

Acknowledgements

The authors gratefully acknowledge the support provided by the Czech Science Foundation under project number GAP 105/12/G059. The authors would like to acknowledge Michaela Kostelecká, from the Klokner Institute, for her assistance with the microscopic investigation of the fibres used in this study. The authors would also like to acknowledge the assistance given by the technical staff of the Experimental Centre, Faculty of Civil Engineering, CTU in Prague, and by students who participated in the project.

References

[1] Millon, O., Riedel, W., Mayrhofer, C., Thoma, K.: *Fiber-reinforced ultra-high performance concrete – a material with potential for protective structures*, Proceedings of the First International Conference of Protective Structures, Manchester, 2010, p. 013.

[2] Máca, P., Sovják, R., Konvalinka, P.: *Mix Design of UHPFRC and its Response to Projectile Impact*, Int. J. Impact Eng., 2013, DOI:10.1016/j.ijimpeng.2013.08.003.

[3] RILEM Draft Recommendation: *Determination of the Fracture Energy of Mortar and Concrete by Means of Three-Point Bend Tests on Notched Beams*, Mater. Struct., **18**, 1985, pp. 285–290.

[4] Bažant, Z. P., Kazemi, M. T.: *Size dependence of concrete fracture energy determined by RILEM work-of-fracture method*, Int. J. Fract., **51**, 1991, pp. 121–138. DOI:10.1007/BF00033974.

[5] Hu, X., Wittmann, F.: *Fracture energy and fracture process zone*, Mater. Struct., **25**, 1992, pp. 319–326. DOI:10.1007/BF02472590.

[6] Maca, P., Zatloukal, J., Konvalinka, P.: *Development of Ultra High Performance Fiber Reinforced Concrete mixture*, IEEE Symposium on Business, Engineering and Industrial Applications (ISBEIA), IEEE, 2012, pp. 861–866. DOI:10.1109/ISBEIA.2012.6423015.

[7] Máca, P., Sovják, R., Konvalinka, P.: *Mixture Design and Testing of Ultra High Performance Fiber Reinforced Concrete*, Malaysian Journal of Civil Engineering, **25 Special Issue (1)**, 2013, pp. 74–87.

[8] Sovják, R., Vogel, F., Beckmann, B.: *Triaxial compressive strength of ultra high performance concrete*, Acta Polytechnica, **53**, 2013, DOI:10.14311/AP.2013.53.0901.

[9] Máca, P., Sovják, R., Vavřiník, T.: *Experimental Investigation of Mechanical Properties of UHPFRC*, Procedia Engineering, **65**, 2013, pp. 14–19. DOI:10.1016/j.proeng.2013.09.004.

[10] Fornůsek, J., Tvarog, M.: Influence of Casting Direction on Fracture Energy of Fiber-Reinforced Cement Composites, Key Eng Mat, 594, 2014, pp. 444–448. DOI:10.4028/www.scientific.net/KEM.594-595.444.

[11] Holčapek, O., Vogel, F., Vavřiník, T., Keppert, M.: *Time Progress of Compressive Strength of High Performance Concrete*, Applied Mechanics and Materials, **486**, 2014, pp. 167–172. DOI:10.4028/www.scientific.net/AMM.486.167.

[12] Li, Q., Reid, S., Wen, H., Telford, A.: *Local impact effects of hard missiles on concrete targets, Int. J. Impact Eng.*, **32**, 2005, pp. 224–284. DOI:10.1016/j.ijimpeng.2005.04.005.

[13] Beckmann, B., Hummeltenberg, A., Weber, T., Curbach, M.: *Strain Behaviour of Concrete Slabs under Impact Load*, Struct. Eng. Int., **22**, 2012, pp. 562–568. DOI:10.2749/101686612X13363929517893.

[14] Banthia, N., Trottier, J.: *Test Methods for Flexural Toughness Characterization of Fiber Reinforced Concrete: Some Concerns and a Proposition*, ACI Mater. J., **92**, 1995, DOI:10.14359/1176.

[15] Birkimer, D. L., Lindemann, R.: *Dynamic tensile strength of concrete materials*, ACI Journal Proceedings, ACI, 1971, DOI:10.14359/11293.

[16] Schuler, H., Mayrhofer, C., Thoma, K.: *Spall experiments for the measurement of the tensile strength and fracture energy of concrete at high strain rates*, Int. J. Impact Eng., **32**, 2006, pp. 1635–1650. DOI:10.1016/j.ijimpeng.2005.01.010.

[17] Tran, T. K., Kim, D. J.: *High strain rate effects on direct tensile behavior of high performance fiber reinforced cementitious composites*, Cement and Concrete Composites, 45, 2014, pp. 186–200. DOI:10.1016/j.cemconcomp.2013.10.005.

[18] Zhang, X., Ruiz, G., Yu, R., Tarifa, M.: *Fracture behaviour of high-strength concrete at a wide range of loading rates*, Int. J. Impact Eng., **36**, 2009, pp. 1204–1209. DOI:10.1016/j.ijimpeng.2009.04.007.